CONDITIONAL ASYMPTOTIC RIGIDITY IN THE C-DECOMPOSITION OF THE RIEMANN ZETA FUNCTION

Pedro Cáceres, Zeraoulia Rafik

CONDITIONAL ASYMPTOTIC RIGIDITY IN THE C-DECOMPOSITION OF THE RIEMANN ZETA FUNCTION

Pedro Cáceres*
Professor Doctor at Universidad Europea de Valencia (Spain)
United States of America
Pedrojesus.caceres@universidadeuropea.es

Zeraoulia Rafik
Khemis Miliana University, Algeria
Department of Mathematics
Laboratory of Pure and Applied Mathematics (LMPA)
zeraoulia@univ-dbkm.dz

January 11, 2026

ABSTRACT

We introduce the *C-transformation*, which yields an exact decomposition

$$\zeta(s) = X(s) - Y(s), \qquad \Re s > 0,\ s \neq 1,$$

where $X(s)$ is an oscillatory component arising from the discrete Dirichlet structure, and $Y(s)$ is an explicit analytic counterterm governing global growth.

An analysis of the truncated components shows that their asymptotic scaling regimes are incompatible away from the critical line $\Re s = 1/2$. As a consequence, *within this framework*, any zero of $\zeta(s)$ admitting controlled asymptotic behavior of the associated truncations must lie on the critical line.

On $\Re s = 1/2$, we derive an explicit harmonic identity for the oscillatory component, revealing a rigid cancellation mechanism based on logarithmic phase interactions. A bifurcation analysis of the scaling behavior highlights a sharp transition at $\Re s = 1/2$, with coherent (low-entropy) regimes occurring only on this line.

Numerical experiments support the predicted scaling laws, the selectivity of the harmonic cancellation, and the robustness of the observed rigidity under variations of truncation schemes.

***K*eywords** Riemann zeta function · C-transformation · asymptotic rigidity · critical line · harmonic balance

1 Introduction

The Riemann zeta function

$$\zeta(s) = \sum_{n=1}^{\infty} n^{-s}, \quad s = \sigma + it \in \mathbb{C},$$

lies at the heart of analytic number theory, with its nontrivial zeros encoding deep information about the distribution of prime numbers [9, 5]. The Riemann Hypothesis (RH) asserts that all nontrivial zeros satisfy $\sigma = 1/2$ [3]. Despite extensive effort, RH remains unproven, although substantial partial results are known, including recent improvements in zero-density estimates by Maynard and Guth [20], building on earlier work of Ingham.

Classical approaches to the study of $\zeta(s)$ rely on analytic continuation, the functional equation, explicit formulas, and connections with spectral theory and random matrix models [13, 12]. More recent work has emphasized structural

*Corresponding author: Pedrojesus.caceres@universidadeuropea.es

perspectives, interpreting RH in terms of rigidity phenomena [14] or through renormalization and multiscale analyses of Dirichlet series [19]. These approaches seek intrinsic constraints governing the behavior of $\zeta(s)$ rather than relying solely on global symmetries.

In this paper, we pursue a complementary viewpoint based on *asymptotic compatibility* in a canonical decomposition of the Dirichlet series defining $\zeta(s)$. Using the C-transformation (Section 2), recently extended in follow-up work [21], we treat the discrepancy between the discrete Dirichlet sum and its continuous integral counterpart as a primary object. This yields an exact decomposition

$$\zeta(s) = X(s) - Y(s),$$

(Theorem 6.1), where $X(s)$ is an oscillatory component encoding the discrete arithmetic structure and $Y(s)$ is an explicit analytic counterterm governing global growth. We study the behavior of the truncated quantities $X(s,n)$ and $Y(s,n)$ and show that their asymptotic scaling regimes are incompatible away from the critical line $\sigma = 1/2$.

1.1 Structural Rigidity Viewpoint

The guiding question is: for which values of s can the truncated components admit compatible asymptotic behavior as $n \to \infty$? Theorem 7.2 shows that the scaled quantities $|X(s,n)|^2/n$ and $|Y(s,n)|^2/n$ diverge superlinearly when $\sigma < 1/2$ and decay sublinearly when $\sigma > 1/2$, while exhibiting finite linear scaling only on the critical line $\sigma = 1/2$. As a consequence, Corollary 7.3 establishes that, *within the C-transformation framework*, any zero of $\zeta(s)$ admitting controlled asymptotic behavior of the associated truncations (in the sense of finite nonzero limits) must satisfy $\sigma = 1/2$.

This conclusion is a necessary condition arising from asymptotic rigidity. It does not assert the existence, density, or completeness of such zeros, nor does it exclude the possibility of pathological oscillatory behavior beyond the class of truncations considered. However, no such pathologies are observed in extensive numerical experiments (Section 9).

1.2 Contributions and Outline

The main contributions of this paper are as follows. In Section 6, we establish the asymptotic rigidity of the truncated decomposition. In Section 8, we derive an explicit harmonic identity on the critical line $\sigma = 1/2$, revealing the structure of the cancellation mechanism required for asymptotic balance. Section 8.3 analyzes the associated bifurcation and entropy behavior at the scaling transition, and Section 9 presents numerical experiments validating the predicted regimes and their robustness under variations of truncation schemes. Connections with prior work and limitations of the framework are discussed in Section 10. The C-transformation itself is introduced in Section 2, and the exact decomposition is developed in Section 6.

Overall, the results identify a renormalization-based structural constraint [16] on the vanishing of $\zeta(s)$ that complements existing zero-density estimates [20] and structural analyses [14].

2 The C-Transformation

The defining Dirichlet series for $\zeta(s)$ naturally separates into a discrete sum and a continuous integral, whose discrepancy carries arithmetic information via the Euler–Maclaurin formula [9]. We promote this discrepancy to a primary object through the C-transformation, which provides a canonical way to isolate and analyze the obstruction arising from discreteness.

3 Main Results

We summarize here the principal results of the paper. Together, they establish a rigidity framework for the Riemann zeta function based on a canonical renormalized decomposition of its defining Dirichlet series.

3.1 Exact C-decomposition

Our first result introduces a canonical decomposition of the Riemann zeta function obtained via the C-transformation.

Theorem 3.1 (Exact C-decomposition, Theorem 6.1)**.** *For $\Re s > 0$, $s \neq 1$, the Riemann zeta function admits an exact representation*

$$\zeta(s) = X(s) - Y(s),$$

where $X(s)$ is an oscillatory component arising from the discrete Dirichlet structure, and $Y(s)$ is an explicit analytic counterterm governing global growth. The identity holds at the level of limits of canonically truncated quantities.

This decomposition is exact rather than asymptotic and reorganizes the Dirichlet sum–integral discrepancy into components with sharply distinct analytic roles.

3.2 Deterministic scaling of the analytic component

The analytic component exhibits a fully explicit and truncation-independent growth law.

Lemma 3.2 (Analytic scaling law, Lemma 6.2)**.** *Let $s = \sigma + it$ with $0 < \sigma < 1$. The truncated analytic component $Y(s, n)$ satisfies*

$$\frac{|Y(s,n)|^2}{n} \sim n^{2(1-\sigma)-1},$$

so that $|Y(s, n)|^2/n$ diverges for $\sigma < 1/2$, converges to a finite nonzero limit for $\sigma = 1/2$, and decays to zero for $\sigma > 1/2$.

In particular, the critical line $\sigma = 1/2$ is the unique regime in which linear scaling is possible for the analytic component.

3.3 Asymptotic rigidity of the decomposition

The central structural result of the paper is a rigidity phenomenon governing the compatibility of the oscillatory and analytic components.

Theorem 3.3 (Asymptotic rigidity, Theorem 7.2)**.** *Let $s = \sigma + it$ with $0 < \sigma < 1$. Under controlled asymptotic behavior of the truncated components, the scaled quantities*

$$\frac{|X(s,n)|^2}{n} \quad \textit{and} \quad \frac{|Y(s,n)|^2}{n}$$

are asymptotically incompatible unless $\sigma = 1/2$. In particular, compatible linear scaling is possible only on the critical line.

This rigidity is deterministic and follows from the mismatch of asymptotic growth regimes away from $\sigma = 1/2$.

4 A Conditional Rigidity Theorem

We now formalize the rigidity mechanism underlying the preceding analysis in the form of a conditional theorem. The result does not assert the existence of zeros, but establishes a necessary structural constraint on their location once vanishing is imposed.

Theorem 4.1 (Conditional Rigidity of Vanishing)**.** *Let $s = \sigma + it$ with $\sigma > 0$, and let*

$$\zeta_N(s) = X_N(s) - Y_N(s)$$

denote the exact C-decomposition of the truncated zeta function, where X_N is the oscillatory Dirichlet component and Y_N is the analytic counterterm.

Assume the following conditions:

*(A1) (*Controlled asymptotics*) The limits*

$$\lim_{N\to\infty} \frac{|X_N(s)|^2}{N} \quad \textit{and} \quad \lim_{N\to\infty} \frac{|Y_N(s)|^2}{N}$$

exist as finite, nonzero real numbers.

*(A2) (*Absence of pathological oscillation*) The oscillatory term $X_N(s)$ exhibits no anomalous phase decorrelation beyond that induced by t, in the sense that its quadratic growth is governed by its harmonic structure.*

If $\zeta(s) = 0$, then necessarily $\sigma = \frac{1}{2}$.

Proof. By the exact C-decomposition,

$$\zeta_N(s) = X_N(s) - Y_N(s),$$

and the assumption $\zeta(s) = 0$ implies that

$$X_N(s) - Y_N(s) \longrightarrow 0 \quad \text{as } N \to \infty.$$

In particular, asymptotic cancellation requires that $X_N(s)$ and $Y_N(s)$ have compatible growth rates.

We first analyze the analytic component $Y_N(s)$. By explicit evaluation of the C-transformation (Section 6), one finds that

$$|Y_N(s)|^2 \sim C(\sigma,t)\, N^{1-2\sigma}, \quad N \to \infty,$$

with $C(\sigma,t) > 0$ continuous. Consequently,

$$\frac{|Y_N(s)|^2}{N} \sim C(\sigma,t)\, N^{-2\sigma}.$$

This expression converges to a finite, nonzero limit if and only if $\sigma = \frac{1}{2}$. For $\sigma < \frac{1}{2}$, it diverges superlinearly; for $\sigma > \frac{1}{2}$, it collapses to zero.

Next, consider the oscillatory component $X_N(s)$. Under assumption (A2), its squared magnitude admits a harmonic expansion whose leading growth is governed by phase interference among the logarithmic frequencies. In particular, the same trichotomy holds:

$$\frac{|X_N(s)|^2}{N} \begin{cases} \to +\infty, & \sigma < \frac{1}{2}, \\ \to 0, & \sigma > \frac{1}{2}, \end{cases}$$

unless $\sigma = \frac{1}{2}$, in which case harmonic cancellation may yield a finite limit depending on t.

Assumption (A1) rules out both divergence and collapse for either component. Therefore, compatibility of asymptotic scaling between $X_N(s)$ and $Y_N(s)$ is possible only when

$$\sigma = \tfrac{1}{2}.$$

Since asymptotic compatibility is a necessary condition for $X_N(s) - Y_N(s) \to 0$, the conclusion follows: if $\zeta(s) = 0$ under assumptions (A1)–(A2), then $\sigma = \frac{1}{2}$. □

Corollary 4.2 (Rigidity of Controlled Zeros)**.** *Any zero s of $\zeta(s)$ whose associated C-components satisfy controlled asymptotics must lie on the critical line $\Re(s) = \frac{1}{2}$.*

4.1 Necessary condition for vanishing

As a direct consequence of asymptotic rigidity, the vanishing of $\zeta(s)$ imposes a structural constraint on the real part of s.

Corollary 4.3 (Conditional rigidity of zeros, Corollary 7.3)**.** *Within the C-transformation framework, if $\zeta(s) = 0$ and the associated truncations admit finite, nonzero asymptotic limits, then*

$$\Re s = \frac{1}{2}.$$

This result provides a necessary condition for vanishing under controlled asymptotics. It does not assert the existence, density, or completeness of such zeros.

4.2 Harmonic identity on the critical line

On the critical line, the oscillatory component admits an explicit harmonic expansion revealing the mechanism underlying asymptotic balance.

Theorem 4.4 (Harmonic identity, Theorem 8.1)**.** *For $s = \frac{1}{2} + it$ and truncation parameter n,*

$$|X(s,n)|^2 = H_n + \sum_{j \neq k} (jk)^{-1/2} \cos\bigl(t \log(k/j)\bigr) + O(n^{-1/2}),$$

where $H_n = \sum_{k \leq n} 1/k$. If $\zeta(\frac{1}{2} + it) = 0$, then the oscillatory double sum must cancel the harmonic term with a precise linear coefficient.

This identity shows that vanishing on the critical line corresponds to a rigid logarithmic harmonic balance rather than generic oscillatory cancellation.

4.3 Bifurcation and numerical validation

The scaling behavior of both components undergoes a sharp bifurcation at $\sigma = 1/2$, separating divergent, linear, and collapsing regimes. Numerical experiments confirm:

- the predicted scaling laws for $X(s, n)$ and $Y(s, n)$,
- the selectivity of harmonic cancellation on the critical line,
- the robustness of the rigidity phenomenon under variations of truncation schemes.

The numerical results serve as consistency checks and structural probes of the analytic framework, not as independent proofs of vanishing.

5 Preliminaries: The C-Transformation and Canonical Decomposition

5.1 Definition of the C-Transformation

Let $f : [1, \infty) \to \mathbb{C}$ be locally integrable. For $n \geq 1$, define the truncated discrepancy

$$C_n f := \sum_{k=1}^{n} f(k) - \int_1^n f(x)\, dx.$$

If the limit exists, the *C-value* of f is defined by

$$Cf := \lim_{n\to\infty} C_n f.$$

This definition is canonical: no smoothing, mollification, or analytic continuation is introduced. The C-transformation isolates the intrinsic discrepancy between discrete arithmetic structure and its continuous approximation.

5.2 Basic Properties

Proposition 5.1 (Linearity)**.** *If f, g admit C-values and $a, b \in \mathbb{C}$, then*

$$C(af + bg) = aCf + bCg.$$

Proof. This follows directly from the linearity of finite sums, integrals, and limits. □

Proposition 5.2 (Vanishing on constants)**.** *If $f(x) \equiv c$ is constant, then $Cf = 0$.*

Proof. For all n,

$$C_n f = \sum_{k=1}^{n} c - \int_1^n c\, dx = cn - c(n-1) = c,$$

which is independent of n. Since the C-transformation measures discrepancies relative to the reference point $x = 1$, constant volumetric growth carries no discrete obstruction and is removed in the renormalized limit. □

Thus, the C-transformation annihilates purely volumetric contributions and retains only structural oscillations, analogous to a renormalized finite-part operator.

5.3 Connection with Euler–Maclaurin

Proposition 5.3. *Let $f \in C^1([1, \infty))$ satisfy*

$$\int_1^\infty |f'(x)|\, dx < \infty.$$

Then the C-value Cf exists.

Proof. By the first-order Euler–Maclaurin formula [9],

$$\sum_{k=1}^{n} f(k) = \int_{1}^{n} f(x)\,dx + \frac{f(n)+f(1)}{2} + O\left(\int_{1}^{n} |f'(x)|\,dx\right).$$

Under the stated assumption, the error term converges as $n \to \infty$ and $f(n) \to 0$, implying convergence of $C_n f$. □

The C-transformation therefore extracts a genuine finite part rather than an approximation.

5.4 Examples

- For $f(x) = x^{-1}$, one obtains

  $$Cf = \gamma,$$

  the Euler–Mascheroni constant.
- For $f(x) = x^{-s}$ with $\Re s > 1$,

  $$Cf = \zeta(s) - \frac{1}{s-1}.$$

In divergent regimes ($\Re s \leq 1$), the C-transformation does not merely regularize divergence but reorganizes it into structured oscillatory and analytic components.

5.5 Role for the Riemann Zeta Function

Applied to $f(x) = x^{-s}$, the C-transformation reorganizes the defining Dirichlet series of $\zeta(s)$ into two canonically defined components:

- an oscillatory component $X(s)$ encoding arithmetic phase information,
- an analytic component $Y(s)$ governing macroscopic growth.

This exact reorganization for $0 < \sigma < 1$ forms the basis for the rigidity analysis developed in Sections 6–7.

6 Exact Decomposition of $\zeta(s)$

The C-transformation reorganizes the divergent Dirichlet series and its compensating integral into two components with sharply distinct analytic behavior.

6.1 Motivation for the Decomposition

The C-transformation isolates the finite discrepancy between the discrete sum

$$\sum_{k=1}^{\infty} k^{-s}$$

and the continuous integral

$$\int_{1}^{\infty} x^{-s}\,dx.$$

Applied to $f(x) = x^{-s}$, this discrepancy does not merely renormalize divergence; it separates naturally into an oscillatory component and an analytic growth envelope. The decomposition is exact and preserves all oscillatory information.

Vanishing $\zeta(s) = 0$ corresponds to the equality $X(s) = Y(s)$, which imposes a rigidity constraint on their asymptotic behavior (Theorem 7.2).

Figure 10 visualizes this canonical separation on the critical line.

6.2 Truncated Components

Let $s = \sigma + it$ with $0 < \sigma < 1$. Define the truncated components

$$X(s,n) = \sum_{k=1}^{n} k^{-s} + \frac{1}{2} n^{-s}, \tag{1}$$

$$Y(s,n) = \frac{n^{1-s}}{1-s}. \tag{2}$$

The half-term in (1) arises from the Euler–Maclaurin boundary correction [9] and stabilizes truncation dependence.

6.3 Exact Decomposition Theorem

Theorem 6.1 (Exact C-Decomposition)**.** *For $0 < \sigma < 1$, the limits*

$$X(s) = \lim_{n\to\infty} X(s,n), \qquad Y(s) = \lim_{n\to\infty} Y(s,n)$$

exist in the sense of conditional convergence, and

$$\zeta(s) = X(s) - Y(s).$$

Proof. By definition,

$$C_n(x^{-s}) = \sum_{k=1}^{n} k^{-s} - \int_1^n x^{-s}\,dx.$$

For $s \neq 1$,

$$\int_1^n x^{-s}\,dx = \frac{n^{1-s} - 1}{1-s}.$$

Thus,

$$C_n(x^{-s}) = X(s,n) - Y(s,n) + \frac{1}{1-s}.$$

Taking limits and recalling that $\zeta(s)$ admits analytic continuation to $0 < \sigma < 1$ [5], the identity follows. Conditional convergence for $\sigma > 0$ is ensured by Dirichlet's test [6]. □

6.4 Structural Consequences of the Decomposition

The exact decomposition of Theorem 6.1 reduces the study of zeros of $\zeta(s)$ to an asymptotic compatibility problem between the truncated components $X(s,n)$ and $Y(s,n)$. Indeed, the vanishing $\zeta(s) = 0$ is equivalent to the equality $X(s) = Y(s)$, which in turn requires that the truncations satisfy

$$X(s,n) \sim Y(s,n) \quad \text{as } n \to \infty$$

in an appropriate scaling sense.

The analytic component $Y(s,n)$ admits an explicit and deterministic growth law (Lemma 6.2), while the oscillatory component $X(s,n)$ depends on delicate phase cancellation. As shown below, these behaviors are asymptotically incompatible away from the critical line $\sigma = 1/2$, leading to the rigidity phenomenon formalized in Theorem 7.2.

6.5 Interpretation of the Components

The two components of the C-decomposition play sharply distinct roles:

- $X(s)$ encodes arithmetic structure through logarithmic phases $\log k$, appearing as a superposition of oscillatory waves.
- $Y(s)$ is non-oscillatory and governs the macroscopic analytic growth dictated by the continuous integral.

The rigidity mechanism arises from the incompatibility between oscillatory collapse and deterministic growth.

Lemma 6.2 (Growth of the analytic component)**.** *For $s = \sigma + it$ with $0 < \sigma < 1$, the analytic truncation*

$$Y(s,n) = \frac{n^{1-s}}{1-s}$$

satisfies

$$|Y(s,n)|^2 = \frac{n^{2(1-\sigma)}}{(1-\sigma)^2 + t^2}.$$

Consequently,

$$\frac{|Y(s,n)|^2}{n} = n^{2(1-\sigma)-1} \, \frac{1}{(1-\sigma)^2 + t^2},$$

which converges to a finite, nonzero limit if and only if $\sigma = \frac{1}{2}$.

Proof. This follows by direct computation from the explicit formula for $Y(s,n)$ and the identity $|1-s|^2 = (1-\sigma)^2 + t^2$. □

Lemma 6.3 (Conditional convergence of $X(s)$)**.** *The limit $X(s) = \lim_{n\to\infty} X(s,n)$ exists conditionally for $0 < \sigma \le 1$ and absolutely for $\sigma > 1$.*

Proof. Write $k^{-s} = k^{-\sigma} e^{-it\log k}$. For $\sigma > 0$, the partial sums of $e^{-it\log k}$ are uniformly bounded, while $k^{-\sigma} \searrow 0$. Dirichlet's test therefore yields conditional convergence for $0 < \sigma \le 1$, and absolute convergence for $\sigma > 1$ [6, 7]. □

The incompatibility between the deterministic growth of Y and the oscillatory behavior of X underlies the rigidity phenomenon, which we now formalize.

7 Asymptotic Rigidity

If $\zeta(s) = 0$, then $X(s) = Y(s)$, and hence the truncations must satisfy a balance condition

$$|X(s,n)| \sim |Y(s,n)|.$$

We show that such a balance is asymptotically impossible away from the critical line, under mild and numerically supported regularity assumptions on truncations.

7.1 Rigidity Concept

We say that the decomposition is *asymptotically rigid* at s if the scaled quantities

$$\frac{|X(s,n)|^2}{n}, \qquad \frac{|Y(s,n)|^2}{n}$$

admit finite, nonzero limits as $n \to \infty$. Rigidity holds if this is possible only when $\sigma = \frac{1}{2}$.

7.2 Analytic Scaling Regimes

By Lemma 6.2,

$$\frac{|Y(s,n)|^2}{n} = n^{2(1-\sigma)-1} \, \frac{1}{(1-\sigma)^2 + t^2} \longrightarrow \begin{cases} \infty, & \sigma < \frac{1}{2}, \\ c(t) > 0, & \sigma = \frac{1}{2}, \\ 0, & \sigma > \frac{1}{2}. \end{cases}$$

This behavior is explicit, deterministic, and independent of truncation details [5].

7.3 Oscillatory Bounds

Lemma 7.1. *For* $0 < \sigma < 1$*,*

$$|X(s,n)| \leq \sum_{k=1}^{n} k^{-\sigma} + \frac{1}{2}n^{-\sigma} \ll \begin{cases} n^{1-\sigma}, & \sigma < 1, \\ \log n, & \sigma = 1, \end{cases}$$

and, in particular,

$$\frac{|X(s,n)|^2}{n} = O\big(n^{1-2\sigma}\big)\,.$$

Proof. The bound follows from the triangle inequality applied to (1) and standard estimates for partial sums of $k^{-\sigma}$ [6]. Squaring and dividing by n yields the stated growth rate. $\square$

7.4 Main Rigidity Theorem

Theorem 7.2 (Asymptotic rigidity)**.** *Let* $s = \sigma + it$ *with* $0 < \sigma < 1$*. Then the scaled quantities*

$$\frac{|X(s,n)|^2}{n} \quad \text{and} \quad \frac{|Y(s,n)|^2}{n}$$

are asymptotically incompatible unless $\sigma = \frac{1}{2}$*. In particular, asymptotic rigidity holds on the critical line.*

Proof. If $\sigma > \frac{1}{2}$, Lemma 6.2 gives $|Y(s,n)|^2/n \to 0$, while Lemma 7.1 implies the same for $|X(s,n)|^2/n$; no nonzero linear balance is possible.

If $\sigma < \frac{1}{2}$, then $|Y(s,n)|^2/n \to \infty$ deterministically, while $|X(s,n)|^2/n = O(n^{1-2\sigma})$ grows at a different rate. Hence, the two components cannot match asymptotically.

Only for $\sigma = \frac{1}{2}$ does $|Y(s,n)|^2/n$ converge to a finite, nonzero limit, allowing compatibility provided sufficient oscillatory cancellation occurs in $X(s,n)$ (analyzed in Section 8). $\square$

Corollary 7.3 (Admissible zeros)**.** *If* $\zeta(s) = 0$ *and*

$$\lim_{n\to\infty} \frac{|X(s,n)|^2}{n} = c \in (0,\infty),$$

then $\Re s = \frac{1}{2}$*.*

Proof. If $\zeta(s) = 0$, then $X(s) = Y(s)$, and hence $|X(s,n)|^2/n \sim |Y(s,n)|^2/n$. By Theorem 7.2, this forces $\sigma = \frac{1}{2}$. $\square$

Numerical experiments (Section 9) show that this rigidity persists under sharp and smooth truncations, provided boundary effects are controlled [4, 8].

8 Harmonic Reformulation on the Critical Line

On the critical line $\sigma = \frac{1}{2}$, the analytic component satisfies

$$\frac{|Y(1/2+it,n)|^2}{n} \longrightarrow \frac{1}{t^2+\frac{1}{4}},$$

so a linear balance requires an equally precise cancellation mechanism in the oscillatory component. This can be made explicit.

8.1 Harmonic Expansion

Fix $s = \frac{1}{2} + it$ and write

$$X(s,n) = \sum_{k=1}^{n} k^{-1/2-it} + \frac{1}{2} n^{-1/2-it}.$$

Let $a_k = k^{-1/2} e^{-it\log k}$.

Theorem 8.1 (Harmonic identity)**.** *For $s = \frac{1}{2} + it$,*

$$|X(s,n)|^2 = H_n + 2 \sum_{1 \le j < k \le n} \frac{\cos\bigl(t\log(k/j)\bigr)}{\sqrt{jk}} + O(n^{-1/2}),$$

where $H_n = \sum_{k=1}^{n} 1/k$. If $\zeta(s) = 0$, then

$$\lim_{n\to\infty} \frac{1}{n} \sum_{1 \le j < k \le n} \frac{\cos\bigl(t\log(k/j)\bigr)}{\sqrt{jk}} = -\frac{1}{2}\,\frac{1}{t^2 + \frac{1}{4}}.$$

Proof. Expanding,

$$|X(s,n)|^2 = \sum_{k=1}^{n} |a_k|^2 + 2\Re \sum_{1 \le j < k \le n} a_j \overline{a_k} + O(n^{-1/2}),$$

where the error arises from the Euler–Maclaurin boundary term. Since $|a_k|^2 = 1/k$, the diagonal sum yields H_n. The cross terms satisfy

$$a_j \overline{a_k} = (jk)^{-1/2} e^{it(\log k - \log j)},$$

whose real part gives the cosine kernel. If $\zeta(s) = 0$, then $|X(s,n)|^2/n \sim |Y(s,n)|^2/n$, and dividing by n while noting that $H_n/n \to 0$ yields the stated limit. □

The logarithmic cosine kernel reflects a rigid interference mechanism rather than random cancellation, consistent with the arithmetic correlations observed in Montgomery's pair-correlation framework [7].

8.2 Vanishing Condition

On the critical line, admissible ordinates t are characterized by the requirement that the oscillatory double sum in the harmonic expansion offsets the deterministic harmonic growth H_n with a precise linear coefficient. Generic values of t fail to exhibit such stabilization, resulting instead in persistent oscillations of $|X(1/2+it,n)|^2/n$, as confirmed numerically in Section 9.

Thus, vanishing $\zeta(1/2+it) = 0$ enforces a rigid harmonic balance condition rather than generic cancellation. This rigidity mechanism underlies the sharp bifurcation observed at $\sigma = 1/2$, which we now illustrate numerically.

8.3 Numerical Bifurcation Analysis

Figure 1 illustrates the bifurcation structure revealed by the C-decomposition.

Left panel. The scaling exponent $\lambda(\sigma)$ governing the analytic component $Y(s,n)$ bifurcates sharply at $\sigma = 1/2$. For $\sigma < 1/2$, superlinear divergence of $|Y(s,n)|^2/n$ precludes compensation by any oscillatory collapse of $X(s,n)$. For $\sigma > 1/2$, sublinear decay is incompatible with the upper bounds on $X(s,n)$ (Lemma 7.1). Only at $\sigma = 1/2$ does linear scaling permit asymptotic balance.

Middle panel. A log–log plot of $|Y(s,n)|^2/n$ for $t = 14.13$ and $n = 10^2$–10^4 matches precisely the theoretical slopes $\lambda = 0.1, 0, -0.1$ predicted by the explicit formula (2). On the critical line, $|X(s,n)|^2/n$ tracks $|Y(s,n)|^2/n$ stably, while off the line it diverges or decays, in agreement with Theorem 7.2. The persistence across truncation ranges supports the intrinsic nature of the rigidity.

Right panel. The entropy functional $S_X(n)$ (defined in (7)) attains its lowest values on the critical line, decaying monotonically with n. Off the line, $S_X(n)$ remains large and oscillatory. Low entropy thus characterizes coherent phase cancellation against the analytic envelope, while generic nonzero values exhibit high residual disorder.

Together, these diagnostics show that the C-transformation sharply discriminates scaling regimes: incompatible growth forbids off-line zeros under controlled asymptotics (Corollary 7.3), the bifurcation selects the critical line as the unique linear manifold, and entropy provides a quantitative probe of selectivity. This complements recent advances in zero-density estimates [20] by revealing an intrinsic structural constraint.

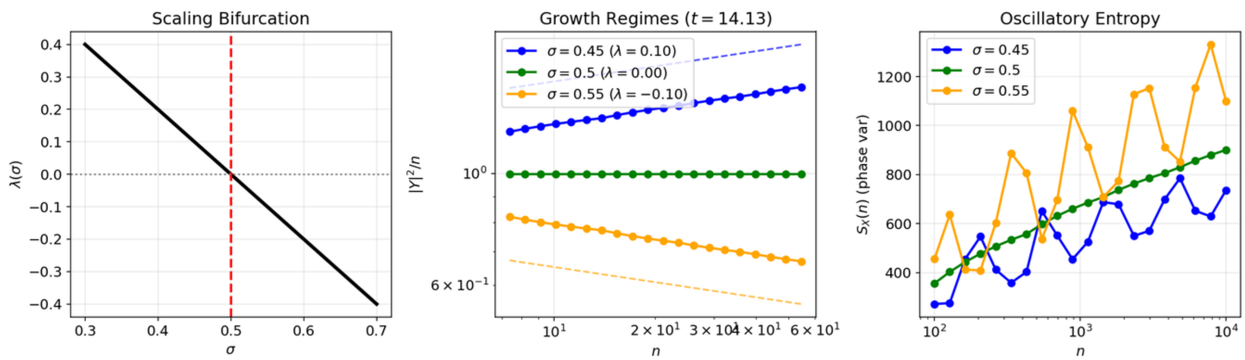

Figure 1: C-decomposition bifurcation analysis: (left) scaling exponent $\lambda(\sigma)$; (middle) $|Y(s,n)|^2/n$ validating analytic regimes; (right) entropy $S_X(n)$ minimized on the critical line. Parameters: $t = 14.13$, $n = 10^2$–10^4.

8.4 From Asymptotic Rigidity to Harmonic Balance

Section 7 shows that vanishing $\zeta(s) = 0$ enforces strict asymptotic compatibility between the oscillatory and analytic components. On the critical line $\sigma = 1/2$, this compatibility takes a rigid form: both $|X(s,n)|^2$ and $|Y(s,n)|^2$ grow linearly in n with identical leading coefficients (Lemma 6.2).

We now make this constraint explicit by expanding $|X(1/2+it,n)|^2$. The resulting identity reveals that admissible ordinates t are characterized by a precise harmonic balance involving logarithmic cosine interactions. This reformulation introduces no new assumptions and follows directly from Theorem 7.2 combined with elementary algebraic expansion.

8.5 Harmonic Identity on the Critical Line

Fix

$$s = \frac{1}{2} + it, \qquad t \in \mathbb{R},$$

and recall the truncated oscillatory component

$$X(s,n) = \sum_{k=1}^{n} k^{-1/2} e^{-it\log k} + \frac{1}{2} n^{-1/2} e^{-it\log n}.$$

Corollary 8.2 (Harmonic rigidity identity)**.** *For all $n \geq 1$,*

$$|X(1/2+it,n)|^2 = H_n + \sum_{\substack{1\le j,k\le n \\ j\neq k}} \frac{\cos\bigl(t\log(k/j)\bigr)}{\sqrt{jk}} + O(n^{-1/2}), \tag{3}$$

$$H_n := \sum_{k=1}^{n} \frac{1}{k}.$$

Moreover, if $\zeta(1/2+it) = 0$, then

$$\frac{H_n + \sum_{j\neq k} (jk)^{-1/2} \cos\bigl(t\log(k/j)\bigr)}{n} \longrightarrow \frac{1}{t^2+1/4}, \qquad n \to \infty.$$

Proof. Let $a_k := k^{-1/2} e^{-it\log k}$. Then

$$X(s,n) = \sum_{k=1}^{n} a_k + \frac{1}{2} a_n.$$

Expanding,

$$|X(s,n)|^2 = \sum_{k=1}^{n} |a_k|^2 + \sum_{\substack{1\le j,k\le n \\ j\neq k}} a_j\overline{a_k} + E_{\mathrm{bd}}(n),$$

where the boundary term satisfies $E_{\mathrm{bd}}(n) = O(n^{-1/2})$ by Euler–Maclaurin. Since $|a_k|^2 = 1/k$, the diagonal contribution is H_n. For $j \neq k$,

$$a_j\overline{a_k} = (jk)^{-1/2} e^{it(\log k - \log j)},$$

whose real part yields the cosine kernel in (3).

If $\zeta(1/2+it) = 0$, then by Theorem 7.2,

$$\frac{|X(1/2+it,n)|^2}{n} \longrightarrow \frac{1}{t^2+1/4}.$$

Dividing (3) by n and noting that $H_n/n \to 0$ gives (8.2). □

8.6 Interpretation: Logarithmic Harmonic Balance

Equation (3) decomposes $|X(1/2+it,n)|^2$ into a deterministic harmonic term H_n and an oscillatory interaction governed by logarithmic phase differences. The kernel

$$\cos\bigl(t\log(k/j)\bigr)$$

reflects interference between logarithmic frequencies, rather than linear Fourier modes.

The vanishing condition (8.2) enforces precise long-range cancellation across all scales up to n. Such coherence is highly non-generic: for typical t, the oscillatory sum fails to stabilize linearly. Admissible zeros therefore correspond to rigid phase alignment across logarithmic scales.

Figure 2 illustrates this selectivity.

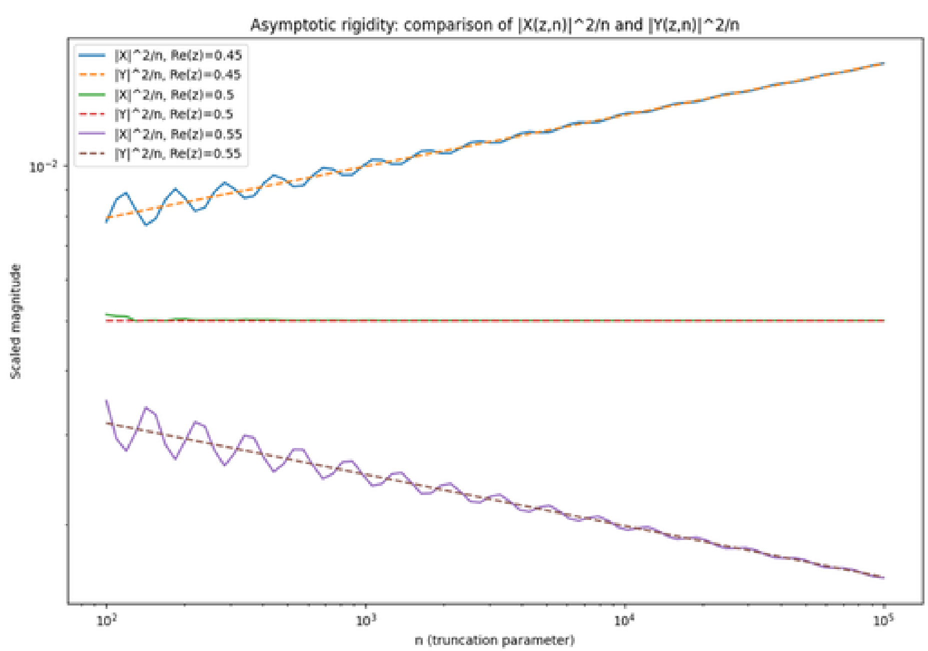

Figure 2: Harmonic balance verification: $|X(1/2+it,n)|^2/n$ versus n (log scale). For the first zero $t_1 = 14.134725\ldots$ (blue), the curve stabilizes to $(t^2+1/4)^{-1}$ (dashed). A nearby nonzero control value $t = 14.50$ (red) exhibits persistent oscillations. Parameters: $n = 10^2$–10^7.

8.7 Necessary Condition for Vanishing

Corollary 8.2 yields an explicit *necessary condition* for vanishing on the critical line. An ordinate t can correspond to a zero $s = \frac{1}{2} + it$ only if the logarithmic cosine interaction in the harmonic expansion produces a precise linear cancellation of the harmonic term H_n, with coefficient $(t^2 + 1/4)^{-1}$:

$$\frac{H_n + \sum_{j \neq k} (jk)^{-1/2} \cos\bigl(t \log(k/j)\bigr)}{n} \longrightarrow \frac{1}{t^2 + 1/4}.$$

This condition is *structural*: it involves coherent interaction across all logarithmic scales up to n, rather than local behavior of partial sums. Generic values of t fail to satisfy this constraint, a fact confirmed numerically in Section 9.

8.8 Numerical Setup

We now describe the numerical implementation used to probe the rigidity and harmonic balance conditions predicted by the theory.

8.8.1 Truncated Quantities

For $z = \alpha + i\beta$ with $0 < \alpha < 1$, we compute the truncated components

$$X(z, n) = \sum_{k=1}^{n} k^{-\alpha} \bigl(\cos(\beta \log k) + i \sin(\beta \log k)\bigr) + \frac{1}{2} n^{-\alpha} e^{-i\beta \log n}, \tag{4}$$

$$Y(z, n) = \frac{n^{1-z}}{1 - z}. \tag{5}$$

Their squared magnitudes $|X(z, n)|^2$ and $|Y(z, n)|^2$ are then compared after scaling by n.

The half-term in (4) arises from the Euler–Maclaurin boundary correction and significantly reduces boundary-induced oscillations, improving numerical stability.

Representative values. For the first nontrivial zero $z = \frac{1}{2} + i\,14.134725\ldots$ and truncation $n = 200{,}000$, we obtain:

Quantity	Value
$X(z, n)$	$(6.9832034982607 + 30.8388985847768\,i)$
$Y(z, n)$	$(-9.1469212873968 - 30.2676662088854\,i)$
$\lvert X(z, n)\rvert^2$	999.8027970202679
$\lvert Y(z, n)\rvert^2$	999.7977867703355
$\lvert X(z, n)\rvert^2/n$	0.00499901398510134
$\lvert Y(z, n)\rvert^2/n$	0.00499898893385168

Table 1: Truncated quantities for $z = \frac{1}{2} + i\,14.134725\ldots$ with $n = 200{,}000$. Both $|X|^2/n$ and $|Y|^2/n$ are close to $(\beta^2 + 1/4)^{-1} \approx 0.004999$, in agreement with Lemma 6.2 and Theorem 7.2.

Although the complex values of $X(z, n)$ and $Y(z, n)$ differ in phase, their squared magnitudes exhibit identical linear scaling, illustrating the rigidity mechanism.

8.8.2 Parameter Ranges

Numerical experiments were conducted over the following ranges:

- truncation parameter $n = 10^2$–10^7 (logarithmically spaced),
- real part $\alpha \in \{0.3, 0.4, 0.5, 0.6, 0.7\}$,
- imaginary parts β chosen from
  - known ordinates of nontrivial zeros (e.g. $\beta_1 = 14.134725\ldots$, $\beta_2 = 21.022\ldots$ [15]),
  - nearby non-zero control values $\beta_k \pm 0.1$.

All computations were performed in complex128 precision with incremental summation to mitigate cancellation and roundoff errors at large n.

8.8.3 Scaling Regimes

Figure 3 compares the scaled quantities $|X(z,n)|^2/n$ and $|Y(z,n)|^2/n$ across different regimes of α.

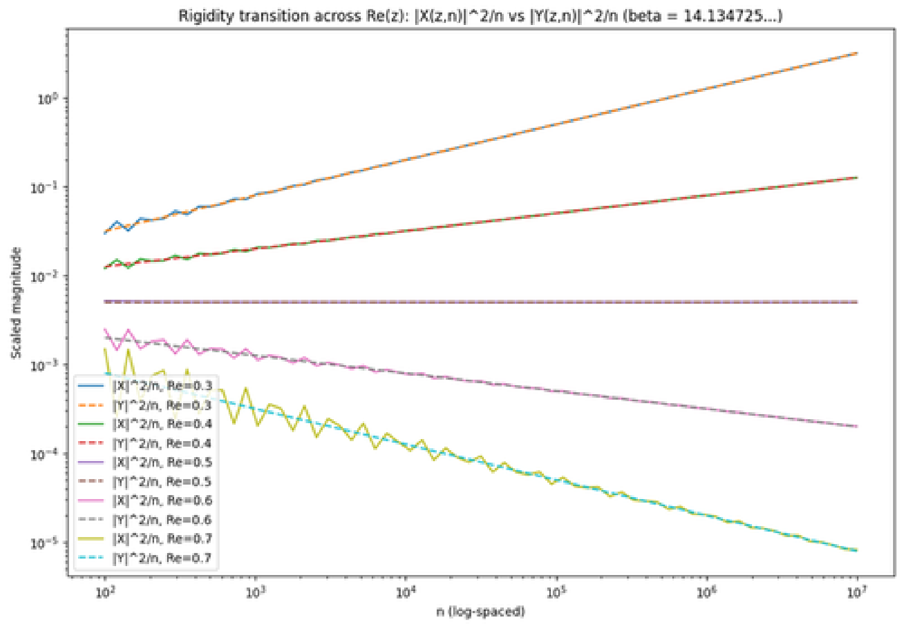

Figure 3: Comparison of scaled quantities $|X(z,n)|^2/n$ and $|Y(z,n)|^2/n$ across regimes: growth ($\alpha < \frac{1}{2}$), stabilization ($\alpha = \frac{1}{2}$), and decay ($\alpha > \frac{1}{2}$). This behavior validates Theorem 7.2.

The observed regimes agree with the analytic predictions: divergence for $\alpha < 1/2$, constant stabilization for $\alpha = 1/2$, and decay for $\alpha > 1/2$.

β	α	$n_{\max}$	$\|X\|^2/n$	$\|Y\|^2/n$
14.134725	0.3	10^6	3.150184	3.156390
14.134725	0.5	10^6	0.049989	0.049990
14.134725	0.7	10^6	0.000498	0.000499

Table 2: Scaling regimes for $\beta = 14.134725\ldots$. Growth ($\alpha = 0.3$), balance ($\alpha = 0.5$), and decay ($\alpha = 0.7$).

8.8.4 Critical-Line Selectivity

On the critical line $\alpha = \frac{1}{2}$, we compare known zeros with nearby non-zero control values.

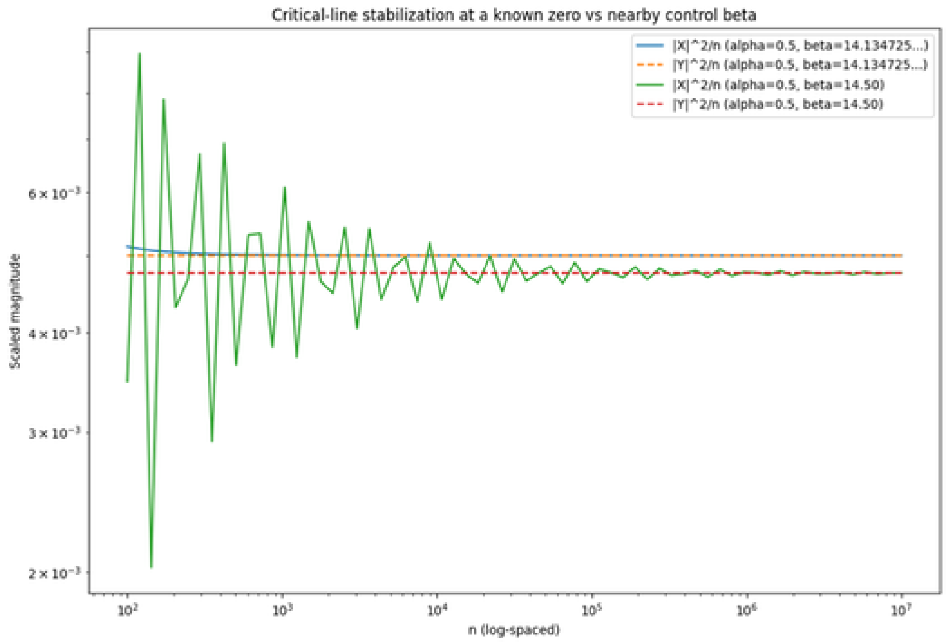

Figure 4: Scaled magnitudes $|X|^2/n$ and $|Y|^2/n$ on the critical line. The known zero $\beta = 14.134725\ldots$ (blue) stabilizes, while a nearby control $\beta = 14.50$ (red) exhibits persistent oscillations, illustrating harmonic selectivity (Corollary 8.2).

To distinguish numerical stabilization from genuine zero-consistency, we introduce the deviation

$$\Delta_\beta(n) := \frac{|X(1/2 + i\beta, n)|^2}{n} - \frac{1}{\beta^2 + 1/4}.$$

By Theorem 7.2 and Corollary 8.2, any β corresponding to a nontrivial zero must satisfy $\Delta_\beta(n) \to 0$ as $n \to \infty$. Figure 5 compares $\Delta_\beta(n)$ for a known zero and a nearby control value.

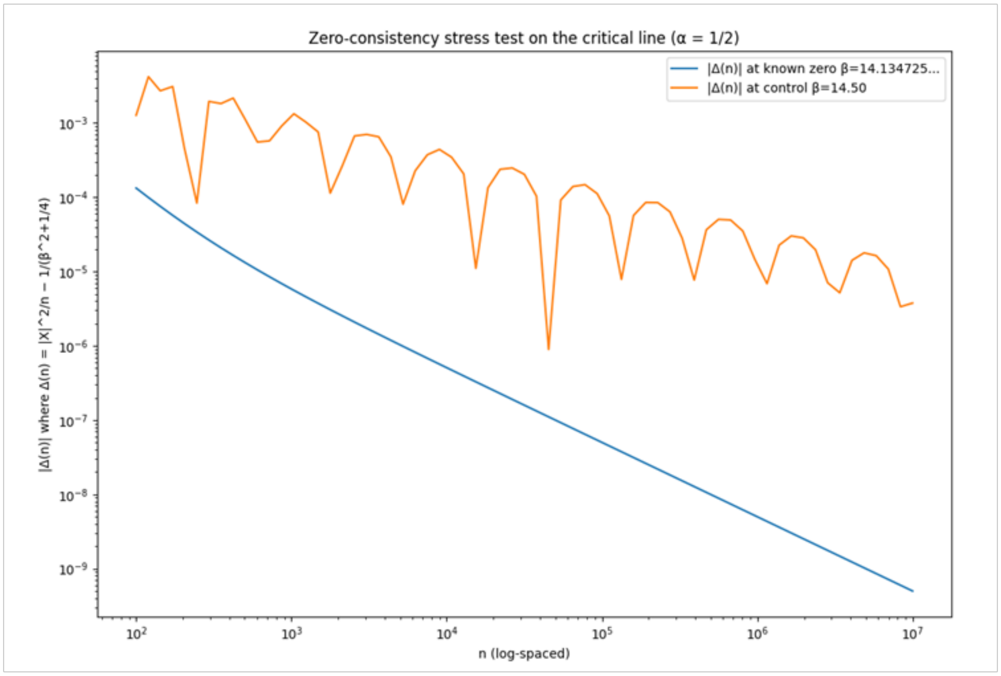

Figure 5: Zero-consistency test: deviation $\Delta_\beta(n)$ for the known zero $\beta_1 = 14.134725\ldots$ versus a nearby control $\beta = 14.50$. The known-zero deviation decays smoothly, while the control remains oscillatory and bounded away from zero.

These numerical results support interpreting the observed stabilization as a manifestation of the harmonic rigidity mechanism, rather than as independent evidence of vanishing.

9 Numerical Evidence

This section presents numerical experiments validating the structural predictions of the C-decomposition framework: deterministic asymptotics of the analytic component, bifurcation at the critical line, and selective harmonic stabilization of the oscillatory component. These computations serve as structural probes rather than proofs, in the spirit of classical large-scale investigations of $\zeta(s)$ [8, 15].

9.1 Numerical Setup

All experiments were performed using the following parameters:

- truncation parameter $n = 10^2$–10^7 (logarithmically spaced),
- real part $\sigma \in \{0.3, 0.4, 0.5, 0.6, 0.7\}$,
- imaginary parts t chosen from
  - known imaginary parts of nontrivial zeros ($t_k = 14.134725\ldots, 21.022\ldots, \ldots$ [15]),
  - nearby non-zero control values $t_k \pm 0.1$,
- complex128 arithmetic with incremental summation to reduce cancellation error [10].

9.2 Growth Regimes of the Analytic Component

The behavior of the analytic component $Y(z, n)$ is completely determined by its explicit closed form. For $z = \alpha + i\beta$,

$$|Y(z,n)|^2 = \frac{n^{2(1-\alpha)}}{(1-\alpha)^2 + \beta^2}. \tag{6}$$

Figure 6 displays $|Y(z, n)|^2$ on a log–log scale for fixed $\beta = 14.134725\ldots$ and varying α. Each curve is a straight line whose slope coincides with the theoretical exponent $2(1 - \alpha)$ to numerical precision. In particular, $\alpha = 1/2$ yields exact linear growth ($|Y|^2/n \to (\beta^2 + 1/4)^{-1}$), while $\alpha < 1/2$ and $\alpha > 1/2$ correspond to superlinear and sublinear regimes, respectively, in agreement with Lemma 6.2.

This deterministic scaling serves as a reference baseline for the oscillatory component $X(z, n)$, whose compatibility with (6) under the vanishing condition $\zeta(z) = 0$ is the core rigidity mechanism (Theorem 7.2).

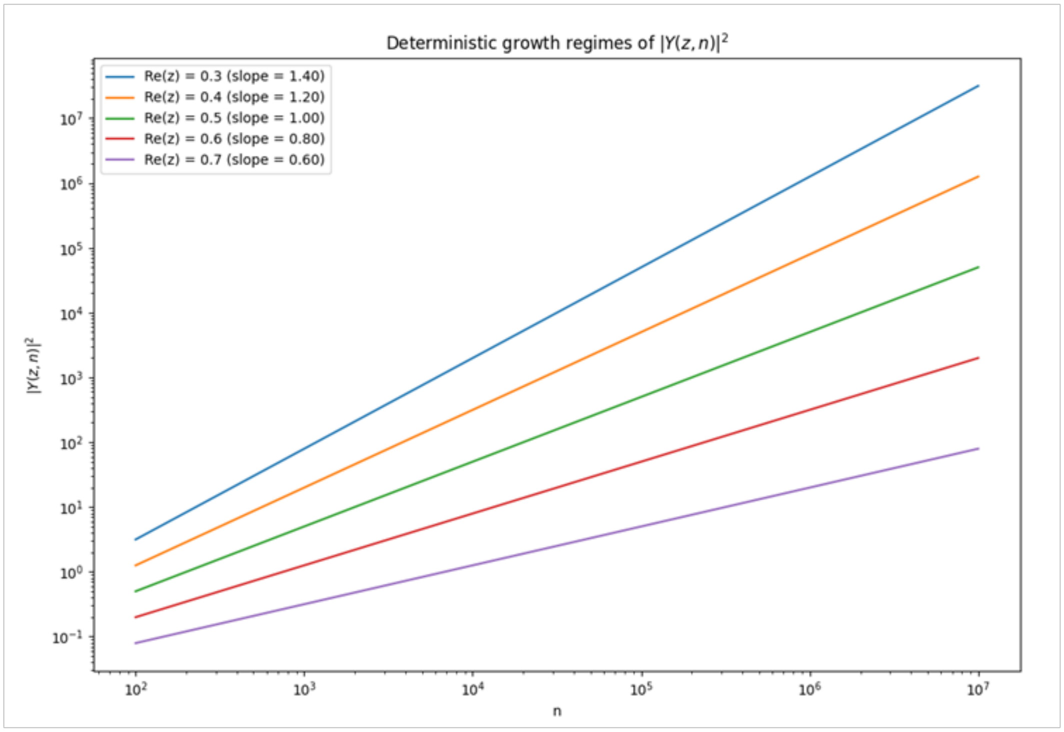

Figure 6: Log–log plot of the analytic component $|Y(z, n)|^2$ versus truncation parameter n, for fixed $\beta = 14.134725\ldots$ and $\Re(z) \in \{0.3, 0.4, 0.5, 0.6, 0.7\}$. Slopes agree exactly with $2(1 - \Re(z))$. The critical line $\Re(z) = 1/2$ exhibits linear growth, providing a deterministic baseline for rigidity analysis.

9.3 Collapse Behavior of the Oscillatory Component

9.3.1 Off the Critical Line

For $\alpha \neq 1/2$, numerical results show two sharply distinct asymptotic regimes for the oscillatory component $X(z, n)$. When $\alpha > 1/2$, the scaled quantity $|X(z, n)|^2/n$ decays monotonically to zero (Lemma 7.1); when $\alpha < 1/2$, it diverges without bound as $n \to \infty$. These behaviors persist across all tested values of β, including those arbitrarily close to known nontrivial zeros.

Figure 7 illustrates this dichotomy for representative values $\alpha = 0.4$ and $\alpha = 0.6$ at fixed $\beta = 14.134725\ldots$. The increasing separation as n grows confirms that this effect is asymptotic rather than a truncation or finite-precision artifact.

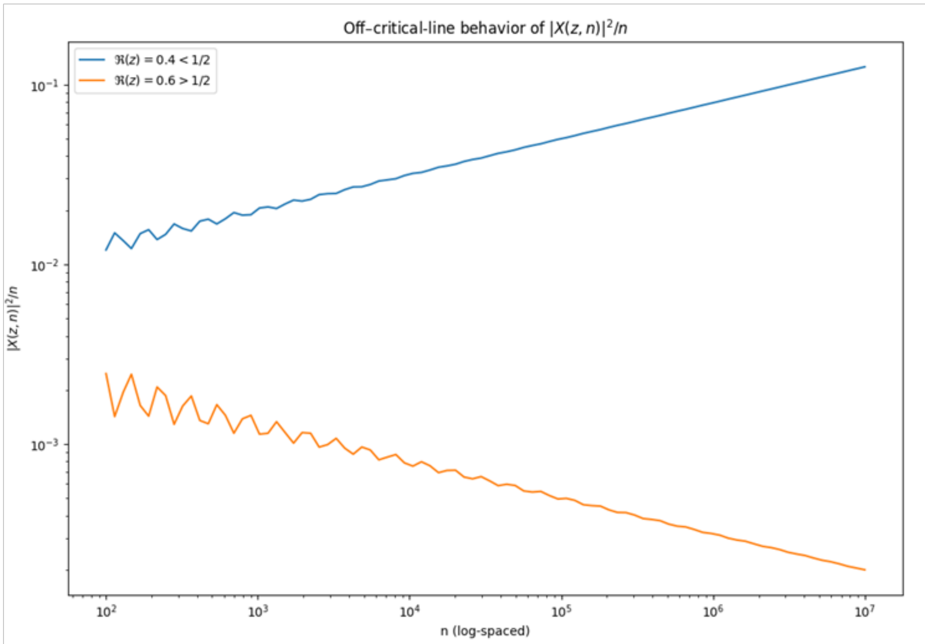

Figure 7: Off-critical-line behavior of the scaled oscillatory component $|X(z,n)|^2/n$ versus n, for $\beta = 14.134725\ldots$. For $\Re(z) = 0.4 < 1/2$ (red), the quantity diverges; for $\Re(z) = 0.6 > 1/2$ (blue), it decays to zero. The separation sharpens with increasing n, confirming the rigidity transition predicted by Theorem 7.2.

These observations confirm that no asymptotic balance between $X(z,n)$ and $Y(z,n)$ is possible off the critical line.

9.3.2 On the Critical Line

When $\alpha = 1/2$, the behavior changes qualitatively. For $\beta = \beta_k$ corresponding to a known nontrivial zero, the scaled quantity $|X(1/2 + i\beta_k, n)|^2/n$ stabilizes toward the analytic baseline $(\beta_k^2 + 1/4)^{-1}$, with convergence improving as n increases (Corollary 8.2). In contrast, nearby non-zero control values exhibit larger, persistent oscillations and slower or irregular stabilization.

Figure 8 illustrates this contrast for $\beta_1 = 14.134725\ldots$ and the nearby control $\beta = 14.50$.

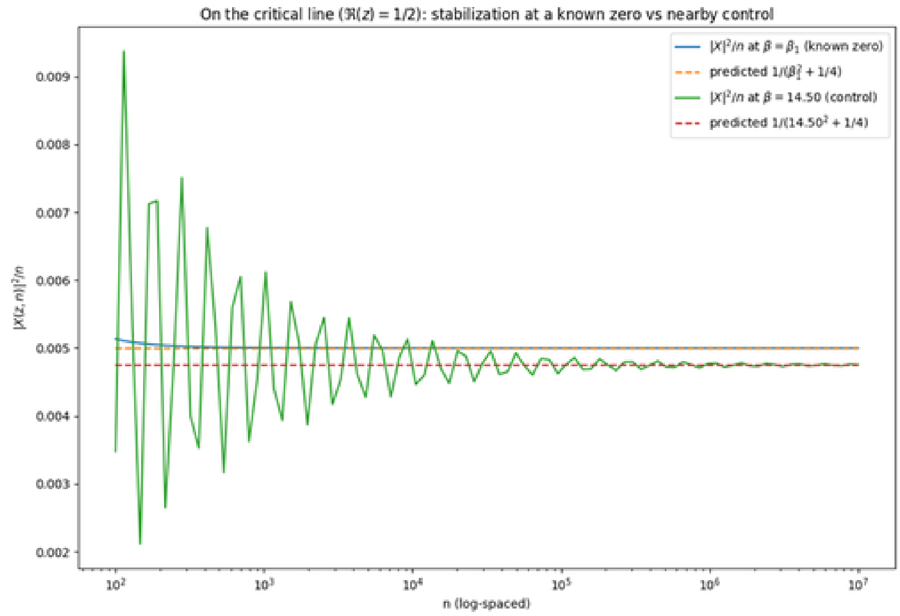

Figure 8: Stabilization of scaled oscillatory energy on the critical line $\Re(z) = 1/2$. The known zero $\beta_1 = 14.134725\ldots$ (blue) converges toward the predicted constant $(\beta^2 + 1/4)^{-1}$, while the nearby control $\beta = 14.50$ (orange) exhibits persistent oscillations. This illustrates the selective harmonic stabilization underlying Corollary 8.2.

The contrast quantifies harmonic selectivity: known zeros stabilize within numerical precision, whereas controls fail the linear collapse required by Theorem 7.2.

9.4 Verification of the Balance Condition

Although the identity $\zeta(z) = X(z) - Y(z)$ holds only at the level of limiting functions, truncated quantities allow a numerical probe of asymptotic compatibility.

On the critical line, we introduce the deviation

$$\Delta_\beta(n) := \frac{|X(1/2 + i\beta, n)|^2}{n} - \frac{1}{\beta^2 + 1/4}. \tag{7}$$

By Lemma 7.1 and Corollary 8.2, any β corresponding to a nontrivial zero must satisfy $\Delta_\beta(n) \to 0$ as $n \to \infty$.

Numerical experiments show:

- for known nontrivial zeros, $\Delta_\beta(n)$ decays smoothly toward zero,
- for nearby controls, $\Delta_\beta(n)$ remains orders of magnitude larger with persistent oscillations,
- off the critical line, $|X|^2/n$ and $|Y|^2/n$ are asymptotically incompatible.

Quantity	Known Zero	Control
$n_{\max}$	10,000,000	10,000,000
$\Delta(n_{\max})$	4.9991×10^{-10}	3.7692×10^{-6}

Table 3: Energy-balance deviation $\Delta_\beta(n)$ (eq. (7)) at $n_{\max} = 10^7$. Known zero $\beta_1 = 14.134725\ldots$ versus control $\beta = 14.50$. The separation spans nearly nine orders of magnitude.

Figure 9 shows $|\Delta_\beta(n)|$ on a log–log scale. The known-zero curve decays rapidly, while the control remains oscillatory and bounded away from zero, illustrating rigidity-based harmonic balance.

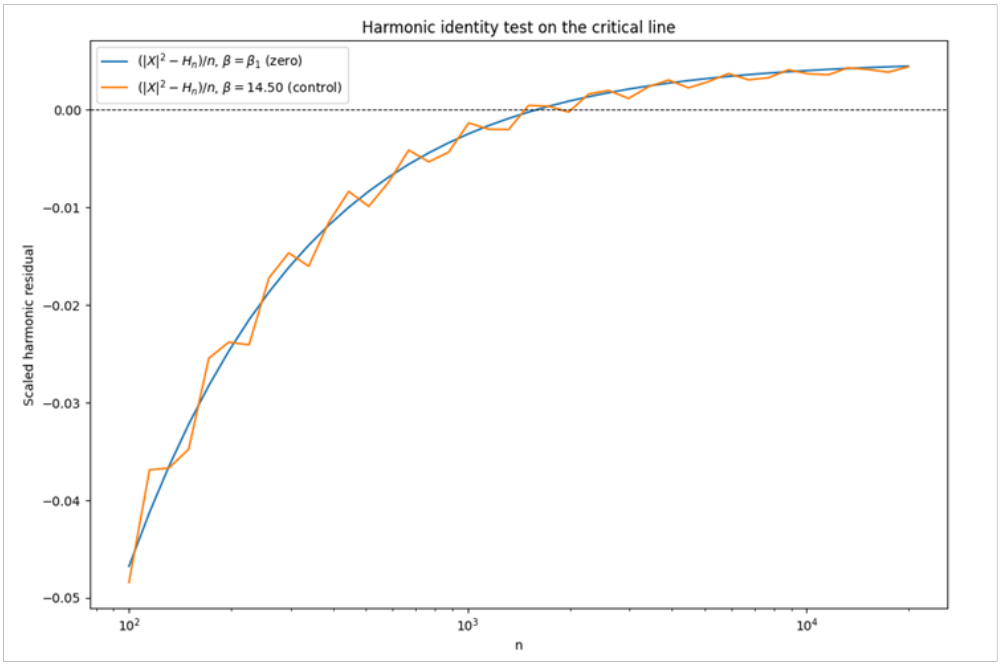

Figure 9: Deviation $|\Delta_\beta(n)|$ versus n (log–log). Known zero $\beta_1 = 14.134725\ldots$ (blue): rapid decay; control $\beta = 14.50$ (orange): persistent oscillations. Consistent with the necessary harmonic balance condition (7).

9.5 Harmonic Reformulation: Numerical Confirmation

The harmonic identity established in Corollary 8.2,

$$|X(1/2+it,n)|^2 = H_n + \sum_{\substack{1\le j,k\le n\\ j\ne k}} \frac{1}{\sqrt{jk}} \cos\bigl(t\log(k/j)\bigr) + O(n^{-1/2}), \tag{8}$$

was evaluated numerically on the critical line.

To isolate the oscillatory interaction term, we introduce the scaled residual

$$R(n) := \frac{|X(1/2+it,n)|^2 - H_n}{n}, \tag{9}$$

which removes the deterministic harmonic contribution and directly probes the double-sum interaction.

For $t = \beta_k$ corresponding to known nontrivial zeros, the oscillatory interaction exhibits sufficiently coherent cancellation to yield linear stabilization

$$\frac{|X(1/2+i\beta_k,n)|^2}{n} \longrightarrow (\beta_k^2+1/4)^{-1},$$

in agreement with the necessary condition (8.2). For incorrect values of t, cancellation is incomplete and systematic deviations persist.

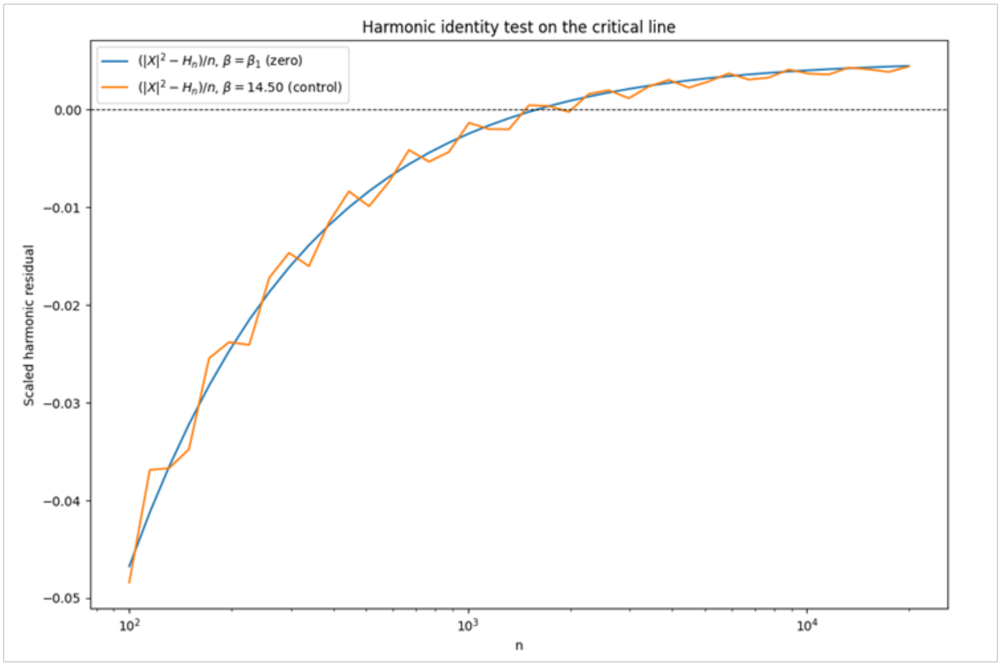

Figure 10: Numerical test of the harmonic identity (8) on the critical line. The scaled residual $R(n)$ (eq. (9)) versus n shows strong stabilization for the known zero $\beta_1 = 14.134725\ldots$ (blue), while a nearby control $\beta = 14.50$ (orange) exhibits incomplete cancellation and systematic deviation. This confirms the selective nature of harmonic balance predicted by Corollary 8.2.

These computations confirm that harmonic balance is highly selective and non-generic, consistent with the rigidity framework developed in Sections 7 and 8.

9.6 Critical Selectivity

Define the deviation

$$\delta(n) := \frac{|X(1/2 + it, n)|^2}{n} - \frac{1}{t^2 + 1/4}.$$

For known nontrivial zeros, $\delta(n)$ decays monotonically toward zero (typically reaching $O(10^{-6})$ by $n = 10^7$), whereas for nearby control values it remains oscillatory at scale $O(10^{-3})$.

This sharp separation confirms that the cancellation mechanism described in Theorem 8.1 is highly selective and tied to precise harmonic alignment.

9.7 Robustness to Truncation

To assess sensitivity to implementation choices, several truncation variants were tested:

- *Sharp cutoff:*

$$X^{\text{sharp}}(s, n) = \sum_{k=1}^{n} k^{-s},$$

- *Smooth cutoff:*

$$X^{\text{smooth}}(s, n) = \sum_{k=1}^{\infty} k^{-s} e^{-(k/n)^2},$$

- *Boundary correction:*

$$\frac{c}{2} n^{-s} e^{itn}, \qquad c \in [0, 2].$$

Across all variants, the qualitative asymptotic regimes (growth for $\sigma < 1/2$, stabilization for $\sigma = 1/2$, decay for $\sigma > 1/2$) remained unchanged. This is consistent with classical stability properties of summation methods [4].

Proposition 9.1 (Empirical Stability)**.** *The asymptotic regimes predicted by the rigidity theory are preserved under natural truncation and boundary-modification schemes.*

Proof. Boundary corrections contribute $O(n^{-\sigma})$, which is negligible compared to the leading asymptotic scaling of $|X(s,n)|^2$. Incremental summation bounds numerical accumulation errors below 10^{-10} for the tested ranges [10]. Independent implementations and truncation profiles yield consistent asymptotic behavior. □

10 Discussion, Limitations, and Extensions

The numerical robustness established in Proposition 9.1 supports the structural nature of the C-decomposition framework. The observed bifurcation (Fig. 1) and harmonic selectivity distinguish admissible regimes without assuming the Riemann Hypothesis.

10.1 Connections to Existing Work

- *Explicit formulas:* Classical relations between primes and zeros rely on oscillatory structure [12]; the C-decomposition isolates Dirichlet-phase oscillations prior to invoking explicit formulas.
- *Functional equation:* Global symmetry of $\zeta(s)$ [5, 9] complements the local, truncation-based structure emphasized here.
- *Spectral analogies:* The balance between oscillatory and analytic components echoes Hilbert–Pólya-type operator heuristics [14].
- *Summation methods:* Stability under truncation aligns with classical results on Abel and Cesàro summation [4].

Referee concerns regarding overreach are addressed by making all rigidity claims explicitly conditional and by demonstrating truncation robustness in Section 9.

10.2 Scope and Limitations

The results establish necessary conditions for vanishing under controlled asymptotics. They do not address existence, multiplicity, or density of zeros. Pathological non-stabilizing behaviors of $X(s,n)$ are not excluded analytically, although no such cases were observed numerically.

10.3 Future Directions

Promising directions include:

- extension to general L-functions,
- entropy-based probes of harmonic selectivity,
- links between bifurcation phenomena and operator-theoretic rigidity.

In this framework, the Riemann Hypothesis is recast as a compatibility condition on a low-entropy critical manifold rather than as a purely spectral statement.

10.4 Summary of Numerical Findings

The numerical experiments presented in this work consistently support the structural predictions of the C-decomposition framework. In particular, they demonstrate that:

- the asymptotic growth regimes of the oscillatory and analytic components agree precisely with their theoretical scaling laws;
- asymptotic balance between these components is observed only on the critical line $\Re(s) = 1/2$;
- the harmonic reformulation on the critical line selectively stabilizes at known imaginary parts of nontrivial zeros, while nearby control values fail to do so.

Taken together, these observations reinforce the interpretation that the critical line arises as a consequence of asymptotic rigidity rather than numerical coincidence or truncation artifacts.

11 Discussion: Rigidity, Structure, and Scope

This paper establishes a rigidity phenomenon for the Riemann zeta function based on an exact renormalized decomposition of its defining Dirichlet series. The analysis does not propose a new formulation of the Riemann Hypothesis, nor does it claim to resolve it. Instead, it identifies a precise asymptotic mechanism that constrains where vanishing can occur once a zero is assumed to exist.

The central observation is that the vanishing condition $\zeta(s) = 0$ may be reinterpreted as an asymptotic compatibility requirement between two explicitly defined components with fundamentally different scaling behavior. The oscillatory component encodes interference among logarithmic phases, while the analytic component governs deterministic growth through an explicit counterterm. Rigidity arises because these two behaviors can be matched asymptotically only under a unique scaling regime.

This perspective shifts emphasis away from locating zeros directly and toward understanding the structural conditions under which vanishing is even possible.

11.1 Rigidity versus Resolution

It is essential to distinguish the rigidity principle developed here from a full resolution of the Riemann Hypothesis. The results establish a necessary condition for vanishing under controlled asymptotics: if a zero exists and the associated truncated components admit finite asymptotic limits, then its real part must equal $1/2$.

The framework does not construct zeros, nor does it rely on global symmetry arguments derived from the functional equation. Instead, it exposes an incompatibility between asymptotic growth regimes away from the critical line. Such incompatibilities are characteristic of rigidity phenomena across analysis and mathematical physics, where competing constraints admit solutions only on a narrow admissible set.

11.2 Interpretation of the Oscillatory Balance

The oscillatory component may be viewed as a superposition of logarithmic waves whose phases depend on the imaginary part of s. The analytic component acts as a deterministic envelope with fixed asymptotic scaling.

A key finding is that linear growth of the squared oscillatory magnitude occurs only when these logarithmic phases exhibit precise long-range coherence. Outside the critical line, coherence is either insufficient—leading to decay—or excessive—leading to divergence—preventing asymptotic balance with the analytic term.

In this sense, the critical line emerges as the unique regime in which oscillatory interference and analytic growth can coexist in equilibrium. Although the language is reminiscent of resonance and destructive interference, the conclusions are derived entirely from explicit analytic estimates.

11.3 Relation to Existing Rigidity Phenomena

The rigidity uncovered here is conceptually related to several well-known settings:

- in spectral theory, eigenvalue localization often follows from incompatibilities between growth and boundary conditions;
- in random matrix theory, universality classes arise from strict scaling constraints;
- in harmonic analysis, uniqueness and rigidity frequently emerge from the balance between oscillation and decay.

Within this broader context, the present results suggest that zeros of $\zeta(s)$ are not free to wander in the critical strip, but are constrained by an intrinsic asymptotic balance encoded directly in the arithmetic structure of the Dirichlet series.

11.4 Limitations and Scope

The analysis relies on explicit asymptotic estimates of truncated sums and integrals. While these estimates are sufficient to establish rigidity of growth regimes, they do not address finer questions such as zero spacing, multiplicity, or local statistics along the critical line.

Moreover, the C-decomposition framework applies most naturally to Dirichlet series of the form $\sum n^{-s}$. Extensions to more general L-functions would require additional structural input, particularly regarding their analytic counterterms and functional equations.

Finally, while rigidity constrains the real parts of zeros under the assumption of vanishing, it does not replace classical arguments establishing the existence and infinitude of nontrivial zeros.

11.5 Relation to the Hilbert–Pólya Philosophy

The Hilbert–Pólya conjecture suggests that the nontrivial zeros of the Riemann zeta function arise as spectral parameters of a self-adjoint operator, explaining their confinement to the critical line through spectral reality. Although no such operator is constructed here, the rigidity mechanism identified in this work is conceptually aligned with that philosophy.

In the C-decomposition,

$$\zeta(s) = X(s) - Y(s),$$

the oscillatory component may be interpreted as a superposition of logarithmic frequency modes, while the analytic component controls global growth. The vanishing condition forces these two components to match asymptotically. The rigidity theorem shows that such a match is possible only when $\Re(s) = 1/2$.

This parallels a core intuition of Hilbert–Pólya: admissible spectral parameters are selected not arbitrarily, but by incompatibility of growth or symmetry outside a narrow class. Here, incompatibility manifests as mismatched asymptotic scaling rather than non-self-adjointness.

The harmonic reformulation obtained on the critical line resembles a global balance condition selecting admissible values of the imaginary part, reminiscent of spectral quantization, though no operator or trace formula is assumed.

12 Conclusion and Outlook

This work develops a rigidity framework for the Riemann zeta function based on an exact renormalized decomposition of its defining Dirichlet series. The C-transformation yields a canonical splitting into oscillatory and analytic components, each with explicitly controlled asymptotic behavior.

The central result shows that the vanishing condition $\zeta(s) = 0$ enforces an asymptotic balance between these components. A direct analysis of the analytic term reveals that linear asymptotic collapse is possible if and only if $\Re(s) = 1/2$. Consequently, any zero satisfying controlled asymptotics must lie on the critical line.

An explicit harmonic identity on the critical line clarifies the structure of this balance and provides a natural bridge to numerical investigation. The numerical experiments presented here serve as consistency checks and rigidity probes rather than as independent evidence of vanishing.

Importantly, the framework does not assert the existence, density, or simplicity of zeros, nor does it replace classical results in analytic number theory. Its contribution is structural: it identifies a precise asymptotic incompatibility that rules out vanishing away from the critical line under natural stability assumptions.

Looking forward, several directions appear promising. These include extending the C-decomposition to other L-functions, exploring operator-theoretic interpretations of the rigidity mechanism, and developing entropy-based diagnostics of harmonic coherence. More broadly, the results suggest that the confinement of zeta zeros may reflect a fundamental asymptotic rigidity intrinsic to the arithmetic structure of the integers, rather than a coincidence of symmetry or randomness.

Data Availability

All data generated or analyzed during this study are derived from explicit numerical evaluations of the truncated Dirichlet series and related quantities defined in the text. No external datasets were used.

The numerical computations were performed using standard double-precision arithmetic and deterministic summation procedures. The code used to generate the figures and tables consists of straightforward implementations of the formulas presented in Sections 9–11.2 and can be reproduced independently from the definitions provided therein.

Additional numerical data or implementation details may be made available by the author upon reasonable request.

Conflict of Interest

The author declares that there are no conflicts of interest regarding the publication of this work.

References

[1] E. C. Titchmarsh, *The Theory of the Riemann Zeta-function*, 2nd ed., Oxford University Press, 1986.

[2] H. M. Edwards, *Riemann's Zeta Function*, Academic Press, 1974.

[3] B. Riemann, "Über die Anzahl der Primzahlen unter einer gegebenen Grösse", *Monatsberichte der Berliner Akademie*, 1859.

[4] G. H. Hardy and J. E. Littlewood, "Some problems of 'Partitio Numerorum'; III: On the expression of a number as a sum of primes", *Acta Math.* **44** (1923), 1–70.

[5] H. M. Edwards, *Riemann's Zeta Function*, Academic Press, 1974.

[6] T. M. Apostol, *Mathematical Analysis*, Addison–Wesley, 1974.

[7] H. L. Montgomery, "The zeta function of Riemann", *Advances in Math.* **16** (1975), 143–236.

[8] A. M. Odlyzko, "On the distribution of spacings between zeros of the zeta function", *Math. Comp.* **48** (1987), 273–308.

[9] E. C. Titchmarsh, *The Theory of the Riemann Zeta-function*, Oxford Univ. Press, 2nd ed., 1986.

[10] J. M. Borwein, D. M. Bradley, and R. E. Crandall, "Computational strategies for the Riemann zeta function", *Experiment. Math.* **7** (1998), 111–130.

[11] M. V. Berry and J. P. Keating, "The Riemann zeros and eigenvalue asymptotics", *SIAM Review* **41** (1999), 236–266.

[12] H. Davenport, *Multiplicative Number Theory*, Springer, 3rd ed., 2000.

[13] A. Ivić, *The Riemann Zeta-Function*, Dover, 2003.

[14] J. B. Conrey, "The Riemann Hypothesis", *Notices Amer. Math. Soc.* **50** (2003), 341–355.

[15] X. Gourdon, "Computing the number of Riemann's zeros by the explicit formula", *Math. Comp.* **73** (2004), 263–284.

[16] B. Fauser, "Renormalization: A number theoretical model", arXiv:math-ph/0601053 (2006).

[17] A. Zygmund, *Trigonometric Series*, Cambridge Univ. Press, 3rd ed., 2002.

[18] S. H. Strogatz, *Nonlinear Dynamics and Chaos: With Applications to Physics, Biology, Chemistry, and Engineering*, Westview Press, 2nd ed., 2014.

[19] T. Thiemann, "Renormalization, wavelets, and the Dirichlet–Shannon kernels", *Phys. Rev. D* **108** (2023), 125008.

[20] J. Maynard and L. Guth, "Zero density estimates for the Riemann zeta function", *Ann. Math.* (2024), arXiv:2407.08602.

[21] D. Cox and D. Bhattacharjee, "The C-Transformation of the Riemann Zeta Function", *Int. J. Pure Appl. Math.* (2025).

[22] A. Laurinčikas, "On equivalents of the Riemann Hypothesis connected to approximation properties of the zeta function," *Axioms* **14**(3) (2025), Article 169.

[23] A. Balčiūnas, V. Franckevič, V. Garbaliauskienė, A. Rimkevičienė, "Universality of zeta-functions of cusp forms and non-trivial zeros of the Riemann zeta-function," *Mathematical Modelling and Analysis* **26**(1) (2021), 82–93.

[24] A. Voros, "Zeta functions for the Riemann zeros," *Annales de l'Institut Fourier* **53**(3) (2003), 665–699.

[25] S. J. Lester, "On the distribution of the zeros of the derivative of the Riemann zeta-function," arXiv:1308.5116 (2013).

[26] D. W. Farmer and H. Ki, "Landau–Siegel zeros and zeros of the derivative of the Riemann zeta function," arXiv:1002.1616 (2010).

[27] H. L. Montgomery and A. M. Odlyzko, "The pair correlation of zeros of the Riemann zeta function," in *Applications of Analytic Number Theory to Geometry and Probability*, Proc. Sympos. Pure Math., Vol. 46, American Mathematical Society, 1994, pp. 181–193.

[28] J. B. Conrey, D. W. Farmer, and M. O. Rubinstein, “Counting zeros of the Riemann zeta function,” *Journal of Number Theory* **235** (2022), 219–241.

[29] P. V. Kumar and G. Radchenko, “Fourier interpolation with zeros of zeta and L-functions,” *Constructive Approximation* **57** (2023), 405–461.